

Where were the monsoon regions and arid zones in Asia prior to the Tibetan Plateau uplift?

Article

Accepted Version

Liu, X., Guo, Q., Guo, Z., Yin, Z.-Y., Dong, B. ORCID: <https://orcid.org/0000-0003-0809-7911> and Smith, R. ORCID: <https://orcid.org/0000-0001-7479-7778> (2015) Where were the monsoon regions and arid zones in Asia prior to the Tibetan Plateau uplift? *National Science Review*, 2 (4). pp. 403-416. ISSN 2053-714X doi: <https://doi.org/10.1093/nsr/nwv068>
Available at <https://centaur.reading.ac.uk/53077/>

It is advisable to refer to the publisher's version if you intend to cite from the work. See [Guidance on citing](#).

Published version at: <http://nsr.oxfordjournals.org/content/2/4/403>

To link to this article DOI: <http://dx.doi.org/10.1093/nsr/nwv068>

Publisher: Oxford University Press

Publisher statement: This is a pre-copyedited, author-produced PDF of an article accepted for publication in *National Science Review* following peer review. The version of record is available online at:

<http://nsr.oxfordjournals.org/content/2/4/403>

All outputs in CentAUR are protected by Intellectual Property Rights law, including copyright law. Copyright and IPR is retained by the creators or other copyright holders. Terms and conditions for use of this material are defined in the [End User Agreement](#).

www.reading.ac.uk/centaur

CentAUR

Central Archive at the University of Reading

Reading's research outputs online

Where were the monsoon regions and arid zones in Asia prior to the Tibetan Plateau uplift?

Xiaodong Liu^{1,2,*}, Qingchun Guo^{1,3}, Zhengtang Guo^{4,2}, Zhi-Yong Yin⁵, Buwen Dong⁶ and Robin Smith⁶

1 SKLLQG, Institute of Earth Environment, Chinese Academy of Sciences, Xi'an, 710075, China

2 CAS Center for Excellence in Tibetan Plateau Earth Sciences, Beijing, 100101, China

3 University of the Chinese Academy of Sciences, Beijing 100049, China

4 KLCGE, Institute of Geology and Geophysics, Chinese Academy of Sciences, Beijing, 100029, China

5 Department of Environmental & Ocean Sciences, University of San Diego, San Diego, 92110, USA

6 National Centre for Atmospheric Science, University of Reading, Reading, RG6 6BB, UK

* Corresponding author: liuxd@loess.llqg.ac.cn

ABSTRACT

The impact of the Tibetan Plateau uplift on the Asian monsoons and inland arid climates is an important but also controversial question in studies of paleoenvironmental change during the Cenozoic. In order to achieve a good understanding of the background for the formation of the Asian monsoons and arid environments, it is necessary to know the characteristics of the distribution of monsoon regions and arid zones in Asia before the plateau uplift. In this study, we discuss in detail the patterns of distribution of the Asian monsoon and arid regions before the plateau uplift on the basis of modeling results without topography from a global coupled atmosphere-ocean general circulation model, compare our results with previous simulation studies and available bio-geological data, and review the uncertainties in the current knowledge. Based on what we know at the moment, tropical monsoon climates existed south of 20°N in South and Southeast Asia before the plateau uplift, while the East Asian monsoon was entirely absent in the extratropics. These tropical monsoons mainly resulted from the seasonal shifts of the Inter-Tropical Convergence Zone. There may have been a quasi-monsoon region in central-southern Siberia. Most of the arid regions in the Asian continent were limited to the latitudes of 20-40°N, corresponding to the range of the subtropical high pressure year-around. In the meantime, the present-day arid regions located in the relatively high latitudes in Central Asia were most likely absent before the plateau uplift. The main results from the above modeling analyses are qualitatively consistent with available bio-geological data. These results highlight the importance of the uplift of the Tibetan Plateau in the Cenozoic evolution of the Asian climate pattern of dry-wet conditions. Future studies should be focused on effects of the changes in land-sea distribution and atmospheric CO₂ concentrations before and after the plateau uplift, and also on cross-comparisons between numerical simulations and geological evidence, so that a comprehensive understanding of the evolution of the Cenozoic paleoenvironments in Asia can be achieved.

INTRODUCTION

The Asian monsoons and arid climates are closely related to global change and, to a large extent, determine the formation and development of various Asian environments [1,2]. The formation and evolution of the Asian monsoon system and inland arid climates have long been a hot topic of Earth's environmental science. With continued accumulation of geological evidence of

43 past climate and advances in the integration and analysis of such records, our knowledge on the
44 timing of establishment of the Asian monsoons and evolution of Asian inland arid climates has
45 improved significantly in recent decades. In terms of the South Asian monsoon (SAM), deep sea
46 drilling records from the Arabian Sea revealed enhanced upwelling around 8 Ma [3], as an
47 indicator of increased southwesterly surface winds. Along with the expansion of C4 plants across
48 the South Asian Subcontinent [4], these records suggested that the establishment or enhancement
49 of the SAM occurred during the late Miocene. However, most geological records related to the
50 SAM have relatively short time-spans, with the longest one lasting approximately 12 Ma up to
51 date [5,6]. Therefore, there is not sufficient evidence regarding the existence or absence of the
52 SAM before the Miocene. In contrast, there is a great abundance of geological evidence on the
53 history of the East Asian monsoon (EAM), which has helped advances in research on the initiation
54 of the EAM. For example, the loess-paleosol sequences from the Chinese loess deposits reflected
55 alternating periods of dominating winter and summer monsoons in East Asia, and thereby
56 indicated the existence of the EAM system since approximately 2.6 Ma [7-9]. The history of the
57 EAM was further extended back to 7-8 Ma during the Pliocene based on the red clay layers
58 beneath the loess and paleosols [9-11]. More recently, studies based on thick eolian deposits in
59 northern China [12,13] and pollen records [14], and reconstructions of evolution of the patterns of
60 paleoenvironments based on geological and geo-biological evidence [15,16] constrained the time
61 of formation of the EAM to 22-25 Ma, during the late Oligocene to early Miocene transition. This
62 conclusion has a profound impact in the study of the Cenozoic environmental change in Asia.

63 In the meantime, the study of the history of Asian inland arid climates has also advanced in
64 the past few decades. Eolian deposits over the Chinese Loess Plateau and those in the Pacific
65 Ocean are good proxies of the aridity of inland Asia and intensity of the atmospheric circulation
66 [12,17,18]. So far the oldest eolian loess deposits have been found to appear during the late
67 Oligocene to early Miocene [12,13,19], but this does not necessarily mean that the Asian inland
68 arid environments formed during this time. In fact, reconstructions of the spatial patterns of
69 paleoenvironments based on bio-geological evidence can better reflect the evolution process of the
70 Asian arid regions than separate geological records at individual locations. By integrating
71 paleobotanical and sedimentary records in China, Sun and Wang [14], Guo *et al.* [15], and Wang
72 *et al.* [16] reconstructed paleoenvironmental patterns during key geological periods. These
73 reconstructions revealed that there was a broad arid zone running from west to east (W-E) across
74 mainland China in the early Tertiary. From the late Tertiary to present, however, the arid climate
75 has been limited mostly to northwestern China. Such changes suggest that at the boundary
76 between the Oligocene and Miocene, the atmospheric circulation over East Asia experienced the
77 shift from a planetary-wind-dominant type to a monsoon-dominated wind system, which disrupted
78 the contiguous zonal pattern of arid regions in Asia and caused corresponding changes in the
79 paleoenvironments. It should also be noted that a recent study by Quan *et al.* [20] suggested that
80 the EAM may have existed during most of the Paleogene (65-23 Ma), which limited the formation
81 of the zonal distribution pattern of arid climates in East Asia. From the above, it can be seen that
82 there are still different views presented in current studies of the Asian paleoenvironments,
83 especially those regarding the timing of the formation of the Asian monsoons, establishment of the
84 subsystems of the Asian monsoons, and the evolution of Asian inland arid climates.

85 Beside geological observations, numerical simulations using 3-D global climate models have
86 become an important approach in studying the evolution of the Asian monsoons and arid

87 environments. In numerical simulations, boundary conditions of atmospheric circulations and/or
88 external forcings can be modified to isolate the effects of various forcing mechanisms and to
89 examine the responses of Asian regional climates to such changes. According to the conventional
90 concept of monsoon climate, monsoon circulation is mainly the product of seasonal variation in
91 land-ocean thermal contrast [21,22]. Numerous simulation experiments have indicated that
92 changes in the land-ocean distribution [23,24] and the uplift of the Tibetan Plateau (TP) [25-27]
93 can have significant impacts on the establishment and evolution of the Asian monsoons. However,
94 other studies suggested that the uplift of the TP only had limited influence on the SAM [28] or that
95 the monsoon is only a result of the seasonal shift of the Inter-Tropical Convergence Zone (ITCZ)
96 [29]. Additionally, numerical simulations have revealed that the uplift of the TP contributed
97 significantly to the formation of the mid-latitude arid climates in Asia [30], although other factors,
98 including the retreat and closing of the Tethys Sea and associated changes in the land-ocean
99 distribution pattern, may have also contributed to the aridification of inland Asia [31,32].

100 Comparisons of the results of numerical simulations with certain geological evidence of the
101 Cenozoic climate change may allow us to qualitatively determine the long-term trends, regional
102 differences, and the forcing mechanisms of climate change in Asia during geological time periods
103 when matching results exist. For example, numerical simulations by Kutzbach *et al.* [26] and Liu
104 and Yin [27] indicated that the TP uplift increased the effects of the plateau as a heat source in
105 summer and heat sink in winter, which amplified the seasonal contrast and enhanced the seasonal
106 shift of the dominant winds in Asia. Therefore, the uplift of the TP enhanced both the Asian
107 winter and summer monsoons. In the meantime, the blocking of moisture by the plateau
108 topography, descending currents caused by the topography-induced stationary wave and dynamic
109 divergent flows from the west to east of the plateau, and the descending air in regions outside the
110 immediate vicinity of the plateau which compensates the rising air above the plateau caused by
111 heating in summer all contributed to the aridification of inland Asia [26,30,33]. These simulation
112 results are qualitatively consistent with the geological records that reflected paleoenvironmental
113 changes during the Cenozoic, with wetting trends in regions south and east of the TP and drying
114 trends in regions west and north of the TP [26,34,35], reflecting the important roles played by the
115 TP uplift in evolution of the Asian climates during the Cenozoic. Also, through model-observation
116 comparisons in studies of the impact of the TP uplift on the formation of the Asian monsoons and
117 inland aridification, it has been recognized that there are still many uncertainties. According to the
118 cumulating geological records over time, the main body of the TP, its margins, and various units
119 of the plateau may have different uplift histories [36-38]. Therefore, the linkages between the
120 history of the plateau uplift and the evolution of the Asian monsoons are not entirely
121 straightforward. For example, An *et al.* [39] suggested that the evolution of the Asian monsoons
122 was coupled with the TP uplift in several stages since the late Miocene, while others have claimed
123 that the Asian monsoons existed in Eocene [40,41], which is earlier than the timing of full-scale
124 uplift of the TP. Several idealized numerical simulations also indicated that the Asian monsoons
125 can be induced by the land-ocean distribution pattern alone without any topography [23,24].
126 Regarding the evolution of arid inland environments in Asia, some geological evidence indicated
127 that arid climates existed in northwestern China since the Tertiary [14,15]. Additionally, at a finer
128 scale, a recent simulation study revealed that the limited uplift of the mountains in the northern TP,
129 including the Pamirs, Tianshan, Kunlun, Altyn-Tagh, and Qilian Mountains, also contributed to
130 the aridification of inland Asia since the Miocene [42].

131 It can be seen from the above that numerous studies have been conducted based on
132 geological records, numerical simulations, or comparisons between the two to examine the
133 formation and evolution of the Asian monsoons and arid inland environments during the Cenozoic.
134 However, different views still exist, especially regarding the impact of the plateau uplift and, if
135 such an impact indeed exists, its magnitude and spatial range. Therefore, it is necessary to obtain
136 the knowledge of the conditions before the TP uplift, so that a focus on the background of the
137 formation of the Asian monsoons and inland arid environments, especially the distribution
138 patterns of the Asian monsoon regions and arid inland arid regions before the TP uplift, is of great
139 scientific significance for achieving a comprehensive understanding of the history of the Asian
140 paleoenvironmental change. Equally important is to understand the roles played by the TP uplift in
141 this process. In this article, we first describe numerical simulation results from a global coupled
142 atmosphere-ocean general circulation model (AOGCM) for scenarios with and without global
143 topography. By integrating a detailed analysis of the current simulation results with comparisons
144 with previous studies, we examine the distribution patterns of the Asian monsoons and arid
145 climates before the TP uplift and then review and discuss relevant issues and associated
146 uncertainties, which allow us to identify some of the problems or issues that are worth further
147 study in the future.

148

149 **RESULTS FROM A COUPLED ATMOSPHERE-OCEAN MODEL**

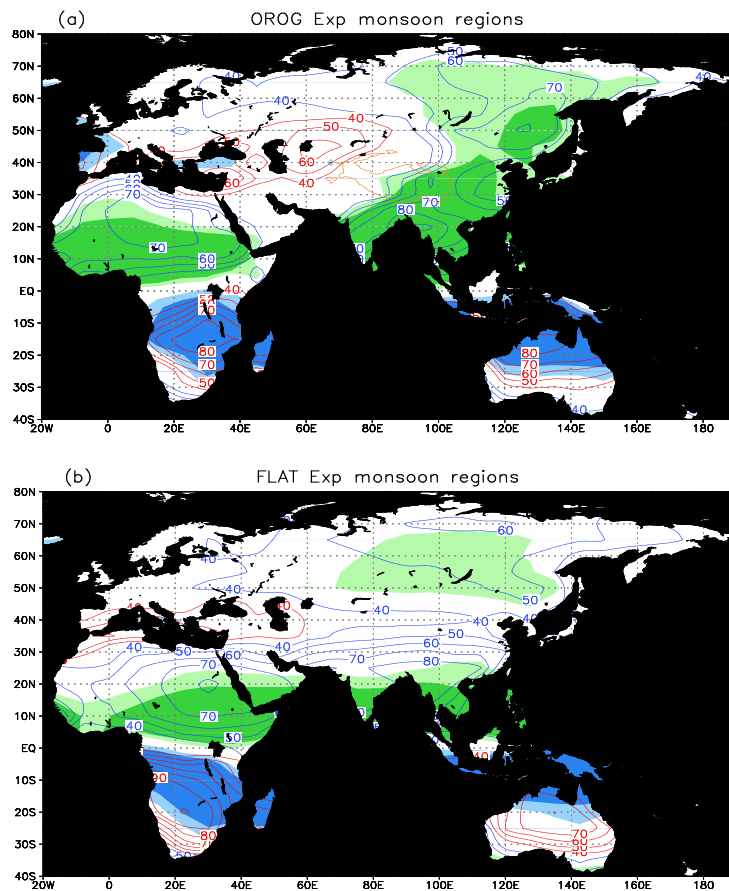
150 We first analyze simulation results from a fully coupled AOGCM by focusing on the spatial
151 distribution patterns of the Asian monsoons and arid zones in a simulation without the global
152 topography and using this analysis as the basis for further discussion and review. The model used
153 in this study is the Fast Met. Office and UK universities Simulator coupled Atmosphere Ocean
154 General Circulation Model (FAMOUS AOGCM) [43,44], which is a low-resolution version of the
155 HadCM3 AOGCM [45]. These AOGCMs do not use flux adjustments. FAMOUS has an
156 atmospheric component with a horizontal resolution of $5^\circ \times 7.5^\circ$, with 11 vertical levels. The
157 ocean component has a horizontal resolution of $2.5^\circ \times 3.75^\circ$, with 20 vertical levels. The
158 atmosphere and ocean are coupled once every day. FAMOUS is structurally almost identical to
159 HadCM3, and produces climate and climate-change simulations that are reasonably similar to
160 HadCM3 but runs much faster. This characteristic is particularly useful for long runs of
161 paleoclimate simulations, for which HadCM3 is too expensive in terms of computing time and
162 resources. More details of the description of FAMOUS and the simulated climates are documented
163 in Smith *et al.* [45,46]. The two experiments described in this study have been run with the
164 standard pre-industrial setup of FAMOUS [45] with an atmospheric CO_2 concentration of 280
165 ppmv. One experiment has the present-day land-ocean mask and topography (abbreviated as
166 “OROG” for the name of the experiment); and the other has the same land-ocean mask and
167 idealized, uniform land surface characteristics as the OROG, but with global orography height set
168 to 0 (abbreviated as “FLAT” for the name of the experiment). Both of these experiments have
169 highly idealized, globally uniform land surface characteristics (albedo, roughness length etc.) to
170 highlight the impact of the orographic changes. Both experiments have been run for 1000 years
171 and the last 100 year mean results are used in this paper. We mainly focus on the distributions of
172 the Asian monsoon regions and arid zones in the following analysis.

173

174 **Asian monsoon regions**

175 The characteristics of precipitation of monsoon climates are mostly reflected in the seasonal
 176 cycle of alternating rainy and dry seasons during the year. In reference to Wang and Ding [47], we
 177 first define the monsoon regions in the Eastern Hemisphere for the OROG and FLAT experiments
 178 using the rainfall seasonality. Specifically, we define monsoon regions as places where the
 179 difference in rainfall between summer (rainy season, as June-July-August (JJA) for Northern
 180 Hemisphere (NH) and December-January-February (DJF) for Southern Hemisphere (SH)) and
 181 winter (dry season, as DJF for NH and JJA for SH) is greater than 200 mm, and where the
 182 percentage of summer to annual total rainfall is greater than 40%. Regions with summer-winter
 183 rainfall difference greater than 400 mm can be considered as the typical monsoon regions. Based
 184 on this definition, for the OROG experiment representing the present-day condition with global
 185 topography (Fig. 1a), the simulated typical monsoon regions are mostly found in the northern
 186

187



188

189 Fig. 1 Distributions of the typical monsoon regions in OROG (a) and FLAT (b) experiments. The
 190 dark (light) green shaded areas indicate where the difference in rainfall between JJA and DJF is
 191 greater than 400 mm (200-400mm). The dark (light) blue shaded areas indicate where the
 192 difference in rainfall between DJF and JJA is greater than 400 mm (200-400mm). The blue (red)
 193 lines show the percentage of JJA (DJF) to annual total rainfall.

194

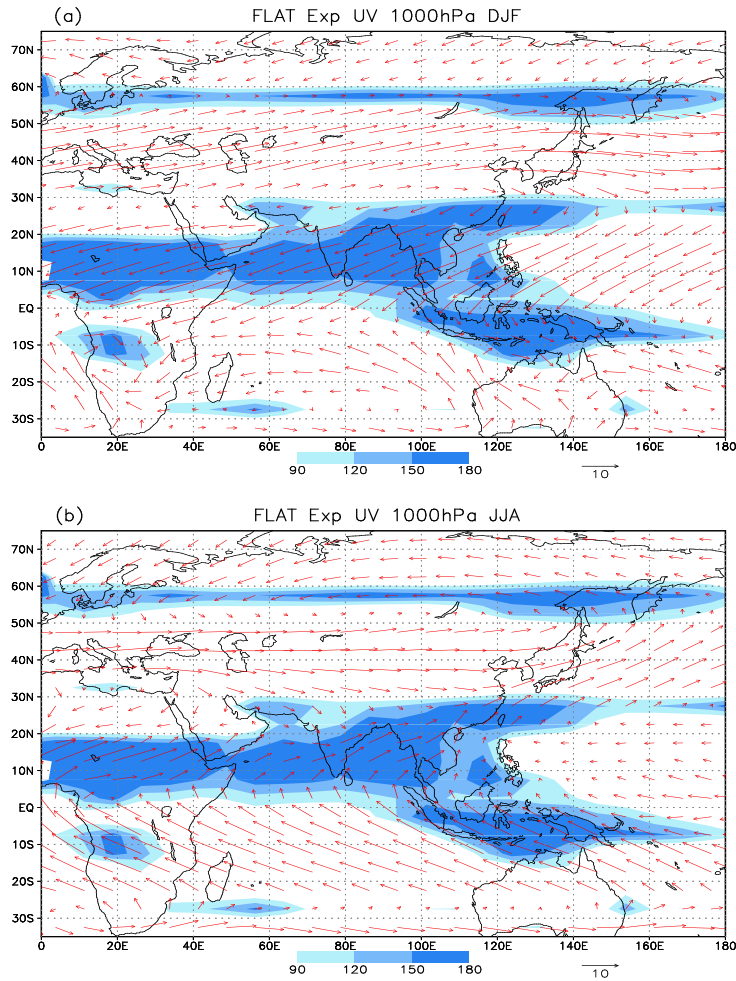
195 tropical Africa (~5-20°N), Indian Subcontinent, Indochina, eastern part of the TP, central and
 196 southern China (east of the TP and south of 40°N) and northeastern China in the NH. In the SH,
 197 typical monsoon regions are found in the southern tropical Africa (~5-20°S) and northern

198 Australia (north of 20°S). For the typical monsoon regions where rainy-dry season rainfall
199 differences are greater than 400 mm, rainy-season rainfall all exceeds 40% of the annual totals and
200 it may reach 70% or higher in the core regions (Fig. 1a). The simulated typical monsoon regions
201 in general match the distribution of the modern monsoon regions in the Eastern Hemisphere as
202 defined by observed precipitation data [47], which indicates good reliability of the model in
203 producing realistic Asian monsoon climates in simulations.

204 Under the condition of zero global topography (Fig. 1b), the monsoon regions simulated by
205 the FLAT experiment are still found in tropical Africa and Australia, although their positions have
206 shifted slightly and spatial extents are somewhat reduced. The greatest changes are found in the
207 Asian monsoon region, where the typical monsoon regions north of 20°N in Fig. 1a have all
208 disappeared in South and East Asia. Fig. 1b shows that the main monsoon regions in Asia are now
209 limited to the Indian subcontinent and central-southern Indochina. This suggests that even without
210 the presence of the TP, the South and Southeast Asian monsoons may still exist, but with reduced
211 intensities and spatial extents, as long as the land-ocean configuration remains the same as today.
212 Additionally, weak monsoon climates can be found in parts of southwestern, southern, and eastern
213 China. It should also be noted that beside the tropical and subtropical monsoons, there exists a
214 quasi-monsoon region in Siberia of the upper mid-latitudes of the Asian continent (~50-65°N)
215 where summer rainfall accounts for 45-60% of the annual total (Fig. 1b).

216 According to the traditional definition of monsoons, they should be characterized by a
217 seasonal reversal of dominating winds [21,48], which lead to wet summers and dry winters. In
218 order to visually interpret the seasonal changes of the dominant winds from the FLAT experiment
219 representing the zero-topography condition, we mapped the simulated NH winter (DJF) and
220 summer (JJA) 1000 hPa wind vectors (Fig. 2). In the NH winter (Fig. 2a), the wind field from
221 Africa to East Asia is very similar to typical planetary wind belts, with the regions south of 30°N
222 mostly being dominated by northeasterly winds. In the NH summer (Fig. 2b), however, the
223 regions south of 20°N from Africa to South and Southeast Asia and those south of 30°N in East
224 Asia are mostly dominated by southwesterly winds. With such seasonal changes in the wind field
225 across the Asian continent, the winter-summer dominant wind direction differences are greater
226 than 120° for the central and southern Indian subcontinent, Indochina, and southern China (south
227 of the Yangtze River) (as shaded areas in Fig. 2). Obviously, these tropical monsoon phenomena
228 as shown in Fig. 1b are attributable to the seasonal oscillation of the ITCZ. We also noted that
229 across the entire Eurasia, there is a narrow W-E running belt north and east of the Lake Baikal
230 with prominent seasonal wind reversal (Fig. 2). This region is located along the northern margin
231 of mid-latitude westerlies in winter, while in summer it is influenced by easterly winds in the
232 northern part of the continental low pressure system. This narrow belt with seasonal reversal of the
233 dominant surface winds matches the aforementioned upper mid-latitude quasi-monsoon belt
234 centered at 55-60°N, defined earlier using seasonality of precipitation.

235 Summarizing the above analysis, based on the seasonal cycles of precipitation and wind, the
236 typical monsoon regions are mostly found in the tropical regions before the TP uplift. Across the
237 Asian continent, typical monsoon climates can be found in the central and southern Indian
238 subcontinent and Indochina, connecting to the weak monsoon regions in southwestern, southern,
239 and eastern China. At the same time, typical monsoon climates can be found in the tropical Africa
240 and northern Australia. Additionally, there might be a narrow zone of quasi-monsoon climate
241 running across the upper mid-latitude Eurasia, especially in central and southern Siberia.



242

243

244

245

246

247

248

Fig. 2 FLAT experiment simulated wind vector fields at 1000 hPa for DJF (a) and JJA (b). The areas shaded are where the absolute value of difference in the mean wind directions between winter and summer is from 90 to 180 degree.

Continental arid zones

249

250

251

252

253

254

255

256

257

258

259

260

261

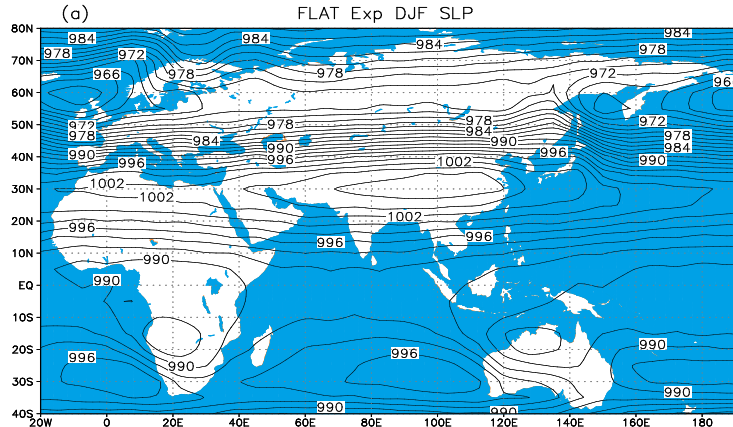
262

263

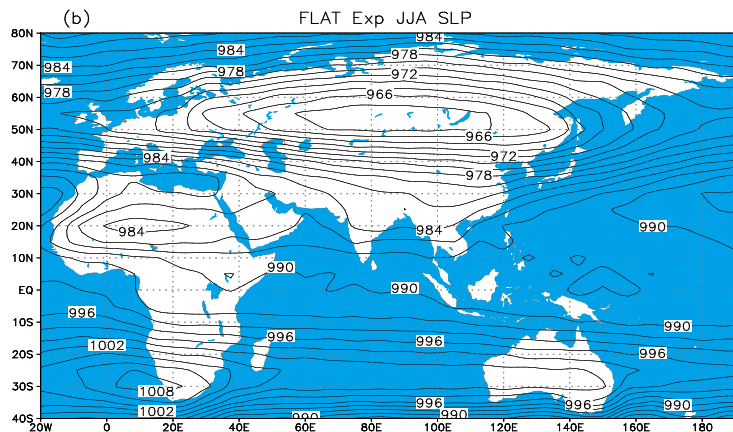
Aridity results from the presence of dry descending air and a lack of moisture, which lead to the lack of clouds and precipitation. Aridity arises from a number of general causes acting individually or working together, for example, atmospheric high pressure zones, continentality, rain shadows, and cold ocean currents [49,50]. At the regional scale, the causes of aridity mainly include continentality that depends on distances from large water bodies or oceans, rain barrier/rain shadow effects of mountains, or cold oceanic surface currents that create stable atmosphere and divert rain-laden air away from coastlines. At the continental or global scale, relatively extensive aridity results from subtropical high-pressure zones related to the downward branches of the Hadley Cells. The descending branches forms zones of elevated sea-level pressure (SLP), referred to as the subtropical high-pressure belts where anticyclonic circulations are persistent [51]. Compression and adiabatic warming of the descending air mass within the high-pressure belts lead to dry and stable atmospheric conditions, eventually promoting development of dryland climates for the regions lying under the anticyclones of the subtropics. Therefore, SLP fields can be used to represent distributions of persistent high-pressure systems and the associated arid climate zones.

264 According to results of the FLAT simulation representing the SLP distribution conditions
 265 before the TP uplift (Fig. 3), there is a zonal pattern of SLP isobars in the NH winter across the
 266 entire Eurasian continent, with SLP values decreasing from the south to north in the mid- to
 267 high-latitude regions north of 30°N (Fig. 3a). This distribution pattern indicates the dominant
 268 control of the westerly circulation in the mid- to high-latitudes with the center of the subtropical
 269 high-pressure zone located close to 30°N from Southwest to East Asia, while the low-pressure

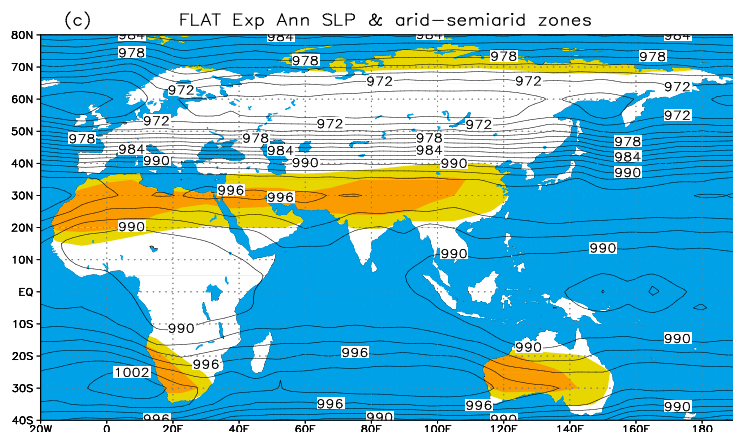
270



271



272



273

274 Fig. 3 FLAT experiment simulated sea level pressure (SLP) fields for DJF (a), JJA (b), and annual
 275 (c) means. The areas of <200mm/a and 200-400mm/a are shaded with brown and yellow colors,
 276 respectively.

277 zone corresponding to the ITCZ is located in the tropical regions south of the equator (Fig. 3a).
278 During the NH summer (Fig. 3b), due to the heating of the Eurasian continent, there is a strong
279 warm-core surface low pressure over the land mass, with the center located near the Lake Baikal
280 at approximately 55°N. This low pressure over land extends to the south and interrupted the
281 continuity of the subtropical-high belt over the Eurasian continent, while over the oceans the
282 northern extent of the subtropical high-pressure cells can reach 40°N or even further north in the
283 Pacific (Fig. 3b). At the same time, the subtropical high-pressure belt in the SH is centered near
284 30°S, extending from southern Africa to central Australia. For the annual average SLP (Fig. 3c),
285 the NH subtropical high-pressure belt extends from North Africa to East Asia, centered near 30°N
286 and there is a low-pressure zone extending W-E centered near 55°N. The latitudes in-between are
287 controlled by the westerlies, while the latitudes north of 55°N are dominated by the polar
288 easterlies. In the SH, the subtropical high-pressure belt is centered near 30°S.

289 According to the comprehensive physical regionalization of China by Zhao [52] and Dry/wet
290 Climate Zoning by Geng *et al.* [53], the simplest criterion to define dry and wet climates is mean
291 annual precipitation (MAP). We define regions with MAP lower than 200 mm as arid and those
292 with MAP of 200-400 mm as semi-arid [52]. Figure 3c shows the distribution of arid and
293 semi-arid regions under the condition of zero topography (FLAT), which are mostly found in a
294 continuous zone between 20°N and 40°N, extending from North Africa to East China, with the
295 core regions near 30°N corresponding to the central location of the NH subtropical high-pressure
296 belt. Zhang *et al.* [54] simulated the Asian climates during the early Eocene and found similar
297 results with an arid zone between 20°N and 40°N. Therefore, it is likely that monsoon climates did
298 not exist in the northern part of South Asia and most of East Asia before the uplift of the TP.
299 Instead of a monsoon circulation, these regions are dominated by widespread and persistent
300 subtropical high pressures and the associated circulation patterns that create the low- to
301 mid-latitude arid zone in Asia. Additionally, arid and semi-arid regions are also found in
302 southwestern South Africa, central and southern Australia, and the northern margin of Eurasia.

303

304 **DISCUSSION AND PERSPECTIVES**

305 In this section, we integrate the above results from the AOGCM simulations with previous
306 relevant simulation and observation studies and discuss the establishment of the Asian monsoons
307 and development of Asian inland arid climates in the Cenozoic. After summarizing the
308 uncertainties in the current knowledge, we will propose some research questions worthy of
309 in-depth study in the future.

310

311 **Formation of the Asian monsoons and inland aridity**

312 From the above experiment of zero global topography in a coupled AOGCM we have
313 inferred distribution patterns of monsoons and arid climates in Asia before the plateau uplift. The
314 simulation results indicate that without global topography, only the tropical monsoons exist in
315 South and Southeast Asia, while the EAM does not exist. These results have validated previous
316 results from atmospheric general circulation models (AGCMs) that the establishment of the SAM
317 is independent of the presence of the TP [28]. Previous studies using AGCMs also revealed that
318 the presence of monsoon precipitation and seasonally reversing wind system in the broad region
319 south of 25°N stretching from the Arabian Sea, to India, Bay of Bengal, and Southeast Asia is
320 clearly evident even without the TP topography [27,55]. Therefore, it is not surprising to find the

321 establishment of monsoon climates in the tropical Asia as early as the Eocene according recent
322 paleoclimate simulations [40,41]. In contrast, the evolution of the EAM is more sensitive to the
323 uplift of the Tibetan Plateau than that of the SAM, especially for the northern part of East Asia
324 [27]. The TP intensifies the EAM, especially through its thermal effects [27,56], and thus its uplift
325 should have played an important role in the formation of the entire Asian monsoon system, but
326 especially for the East Asian component. Our results indicate that, if monsoon climates existed in
327 regions north of the Yangtze River in East Asia in the Eocene or even earlier as suggested by
328 Quan *et al.* [20,57], then the premise should be that the TP uplift must have already occurred and
329 achieved a considerable scale and height at that time. Since the uplift of TP is a complex and
330 diachronous process [58,59], its impact on different sub-systems of the Asian monsoon system is
331 also variable [60] and requires further study. However, at this moment, the 3-D paleoelevation
332 data of the TP since Paleogene and quantitative records of the East Asian peleoenvironments are
333 still sketchy. Even for the limited amount of geological records available, some cannot be fully
334 cross-validated among themselves, due to low temporal resolutions and difficulties in dating
335 [20,38,61-63], or with numerical simulation results (see the last paragraph of this paper).

336 It is worth noting that there may have been a narrow quasi-monsoon zone running across the
337 upper mid-latitude Eurasia (50-65°N), especially in central and southern Siberia before the TP
338 uplift according to our simulation results (Fig. 1b). This region is characterized by a summer rainy
339 season with prominent seasonality. In its core region at 55-60°N, the directions of the winter and
340 summer dominating winds are nearly opposite (Fig. 2), fitting the traditional definition of the
341 monsoon climate. Therefore, to certain extent this region can be considered as having a weak
342 monsoon climate. However, it should be pointed out that at these relatively high latitudes, the
343 winds that bring moisture to produce summer precipitation are not originated from the tropical
344 oceans and have no direct connections to the low-latitude and SH circulations. Thus, such a
345 quasi-monsoon climate is different in nature from the conventional monsoon climates in tropical
346 and subtropical regions. However, this feature of quasi-monsoon climate needs to be further
347 defined, as there is no geological data are yet available to support such a model phenomenon.

348 Under our simulated conditions of zero global topography, the 20-40°N latitudes in the
349 Eastern Hemisphere are under the influence of subtropical high-pressure belt year-around, which
350 causes the formation of the W-E running arid zone. This distribution pattern of the arid climate has
351 been supported by geological evidence indicating that broad zonal arid regions existed across the
352 mainland China in early Tertiary [14,15], while in inland Asia, dry climates prevailed during the
353 long geological period of Eocene to Oligocene [64-66]. The regions south of the subtropical arid
354 zone are mainly controlled by the tropical monsoons, while the latitudes north are dominated by
355 the westerly circulation. In our simulation results, there is no arid climate in the inland Asia north
356 of 40°N, which is similar to previous simulation results by AGCMs [30,67]. This means that,
357 according to numerical simulation results, arid regions did not exist in mid- to high-latitudes of
358 Central Asia before the TP uplift. The characteristics of the actual present-day landforms, however,
359 show that most deserts in Central Asia, Republic of Mongolia, and northern China are located in
360 40°N or higher latitudes. Even with the convincing results from simulation studies pointing to the
361 TP uplift as the major cause of the aridification of Central Asia, the actual climate events during
362 the drying process of Asian inland need further investigation. For example, based on geological
363 records from a terrestrial site (~48°N) in the Junggar Basin in the Asian interior, an evident
364 aridification event at the Eocene–Oligocene Boundary was attributed to global cooling rather than

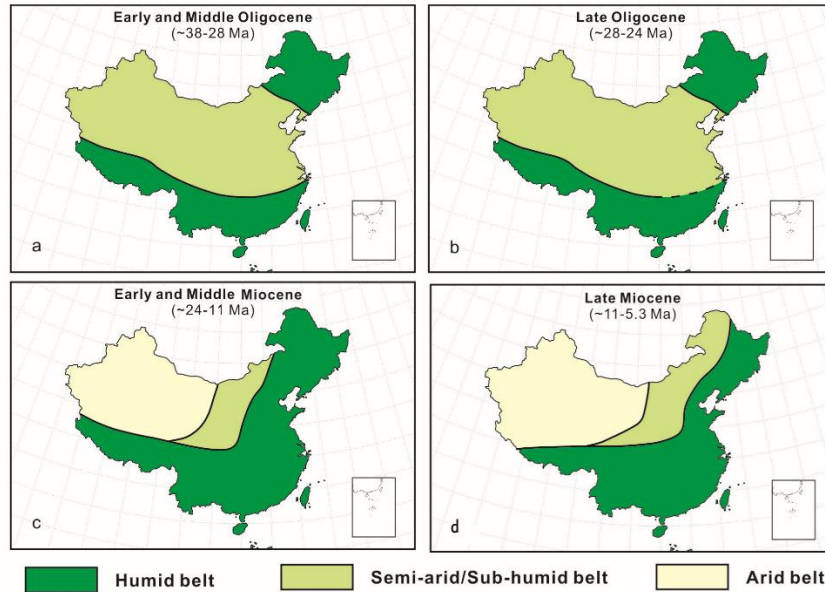
365 regional tectonic uplift [68]. However, the aridity of the Junggar Basin could not have existed
366 without its specific geography and topography in the region and its vicinity. Therefore, the TP
367 uplift, especially the uplift of the northern Tibetan Plateau [42], may have an inherent relation to
368 the formation of the arid regions north of 40°N in Central Asia, the emergence of inland deserts in
369 North China, and enhanced dust cycles in these regions during the Cenozoic.

370 **Comparisons with bio-geological data**

371 Our numerical experiments, thus, have generated some clear insights with regards to the
372 Cenozoic evolution of the Asian climate pattern of dry-wet conditions. Prior to the TP uplift,
373 typical monsoonal climates are only found in the tropical regions. Across the Asian continent,
374 monsoons prevail in the central and southern Indian subcontinent and Indochina, connecting to the
375 weak monsoon regions in southwestern, southern, and eastern China (Fig. 1b). Typical monsoons
376 are also found in the tropical Africa and northern Australia. These monsoon phenomena have been
377 resulted from the insolation-induced seasonal shifts of the ITCZ. On the contrary, a
378 similar-to-present monsoon pattern is observed in the model outputs corresponding to a
379 modern-topography scenario with an elevated Tibetan Plateau (Fig. 1a). These results are highly
380 consistent with the available geological evidence in South Asia (e.g., [69,70]) and reconstructions
381 of the Cenozoic paleoenvironmental patterns based on bio-geological data from China
382 [14,15,71,72]. Sediment records from northeastern India show that the SAM was already
383 established by the late Oligocene with an intensity similar to that of today [69]. The fossil wood of
384 Myanmar also shows that the Bengal Bay experienced a significant monsoonal regime as early as
385 40 Ma ago [70]. The monsoonal regions in the low-latitudes prior to the TP uplift, as shown in our
386 experiments (Fig. 1b), are consistent with the relatively humid conditions in southern China from
387 the Paleogene to the Oligocene as documented by the bio-geological data [14,15] (Fig. 4a,b).
388 Because the cause of these low-latitude monsoons is attributed to the seasonal oscillation of the
389 ITCZ, their presence could be traced back to the very early Earth history when these low-latitude
390 land masses drifted to the present latitudinal positions [15].

391 As for the Asian drylands under the condition of zero global topography, our experiments
392 show a roughly zonal and continuous arid and semi-arid belt prior to the TP uplift, which is
393 located between 20°N and 40°N extending from North Africa to East China, with the core regions
394 near 30°N. This dry belt is clearly attributable to the NH subtropical high-pressure zone. In
395 contrast, such a continental low-latitude dry belt disappears in the scenario after the TP uplift.
396 Meanwhile, central Asia including northwestern China becomes drier. The dry conditions in
397 central Asia after the TP uplift are no longer linked with the subtropical high. The simulated zonal
398 dry belt before the TP uplift (Fig. 3c) is highly consistent with the semi-arid zone defined by the
399 bio-geological indicators with Paleogene ages within China (Fig. 4a,b) [14,15]. The somewhat
400 boarder dry belt shown by the bio-geological data may be caused by the latitudinal shifts of the
401 dry zone in response to the changing global boundary conditions, such that the actual dry belt at
402 any given time should be narrower [15]. This kind of aridity distribution, referred to as
403 “planetary-type dry lands”, is linkable without any doubts with the NH subtropical high-pressure
404 zone. Given that the presence of the subtropical high is relatively independent of any specific
405 topography conditions, such distribution of aridity could also be traced back to much earlier
406 history of the Earth when continents were present in the subtropical latitudes [15].

407



408

409 Fig. 4. Paleoenvironmental patterns during the Oligocene and Miocene in China (modified and
 410 simplified after Guo *et al.* [15]): (a) Early and Middle Oligocene; (b) Late Oligocene (with dashed
 411 line indicating the uncertainty for defining the southeastern boundary between the arid/semi-arid
 412 belt and the humid belt owing to insufficient data); (c) Early and Middle Miocene; and (d) Late
 413 Miocene.
 414

415 The results of numerical experiments in this study for the scenario with global topography are
 416 also in agreements with the Cenozoic paleoenvironmental patterns (Fig. 4) [14,15]. The most
 417 prominent features in our model outputs include the reinforced Asian summer monsoon
 418 circulations prevailing in the low- and mid-latitudes of Asia and expanded monsoon regions over
 419 East Asia (Fig. 1a). This is strongly supported by the bio-geological data [15] showing a drastic
 420 humidification in eastern China since the early Neogene (Fig. 4c). Similarly, the simulated dry
 421 climate in central Asia is consistent with the dry conditions documented by the bio-geological data
 422 [14,15]. Thus the spatial configurations of the monsoon and arid regions are highly comparable in
 423 shape with the modern climate pattern in Asia. The disappearance of the subtropical aridity in East
 424 Asia after the TP uplift is clearly attributable to the northward development of the EAM with the
 425 TP uplift. Although our current study has not taken into account the roles of land-sea distributions,
 426 changing CO₂ concentrations and other possible global boundary conditions, it provides clear
 427 insights to the important roles of the TP uplift in the formations of the monsoon-dominated
 428 climates and inland deserts in Asia. Thus, from both modeling and bio-geological data
 429 perspectives, the low-latitude monsoons prior to the TP uplift are conceptually different from the
 430 present-day Asian monsoons that prevail not only in the low-latitude continents, but also in the
 431 mid-latitude Asia close to the position of the NH westerlies. Similarly, the subtropical high
 432 controlled aridity in Asia before the TP uplift also radically differs, in both origin and concept,
 433 from the present-day dry lands in central Asia, which are independent of the subtropical high. Our
 434 results suggest that any studies of the subject should consider these crucial conceptual differences.
 435 Otherwise, controversies could arise simply because the discussed concepts of the monsoons and
 436 aridity are different.

437 The timing of this drastic climate transition, from a zonal pattern to the similar-to-present
438 patterns over the Asian continent has also drawn much attention from the paleoclimate community.
439 Our model outputs, in association with the geological data, may provide a significant insight to
440 this issue. Although modeling results themselves are not actual chronological events, geological
441 data (Fig. 4) indicate that this major transition would have occurred near the Miocene/Oligocene
442 boundary, between 22 and 25 Ma [11,14,15]. From a temporal perspective, the Miocene loess-soil
443 sequences in northern China [11,12,15] are strong evidence of the presence of monsoon-
444 dominated climates in East Asia back to the early Miocene, as the loess layers attest to the
445 presence of circulation patterns that brought eolian dust from the deserts of interior Asia, while the
446 clay-leached paleosols are firm evidence of more humid conditions with circulation patterns that
447 brought moisture from the oceans [11,15]. These two phases of circulation patterns might be in
448 presence at the same time but alternating seasonally with different directions, rightfully defining a
449 monsoonal climate pattern at least by the early Miocene. The mapping of bio-geological data by
450 different authors [14,15,72] consistently showed that the Oligocene environmental patterns
451 remained zonal but the Miocene patterns, especially the one for the early Miocene (Fig. 4) [15],
452 were already similar to the present-day pattern. These maps tend to constrain the major transition
453 of climate to the Miocene/Oligocene boundary in age, approximately 22-25 Ma. This transition of
454 the paleoenvironmental pattern marks the establishment of the monsoon climates over East Asia
455 north of about 30°N in the early Miocene, which can be used as important evidence against the
456 views of earlier or later EAM establishment. The main challenge for the views about an earlier
457 EAM establishment, for example, the Eocene monsoon [41], would be the zonal climate pattern
458 defined by the Eocene geological data. In contrast, the similar-to-present-day environment pattern
459 since the early Miocene [15] and the loess-soil sequences in northern China would negate the
460 views of a much later EAM establishment.

461 The history of establishment and development of the SAM has not been entirely clear from
462 geological observations, and thus it is difficult to conduct a comprehensive model-observation
463 comparison. Most geological records of the SAM have relatively short time spans, except at few
464 sites where the history of the monsoon can be traced back to the late Oligocene [69] or the late
465 Eocene [70], before the large-scale uplift of the TP or for a period with low topography in general.
466 Up to date no marine records have been obtained to reflect an early existence (prior to the
467 Miocene) of the SAM, although tropical monsoons related to the seasonal oscillation of the ITCZ
468 should have existed before the TP uplift according to numerical simulations. A recent study based
469 on stable carbon isotope records of benthic foraminifera from the Arabian Sea proposed that the
470 present-day SAM wind system began to develop during the late Middle Miocene (~12.9Ma) and
471 the summer monsoon was in its full strength in the late Miocene (~7 Ma) [6]. However, the
472 middle or late Miocene should be regarded as a period of intensification rather than initiation of
473 the SAM. Evidently, the major episodes of strengthening of the SAM in mid-late Miocene [3,4,6]
474 may not have a direct link to the uplift of main body of the TP, an event far before the Miocene
475 [37,38,73]. Additionally, the climatic significance of the proxies for the SAM needs further
476 exploration. For example, the late Miocene Indian Ocean high-productivity event estimated using
477 benthic foraminiferal data, which was originally linked to intensification of the SAM, may be
478 attributed to the Antarctic glaciation and global cooling [74]. A recent oceanography study [75]
479 did not revealed any significant sea surface temperature changes in the Arabian Sea, a crucial
480 criterion previously used by Kroon *et al.* [3] to define the reinforced SAM.

481 **Current uncertainties and further issues**

482 It should be noted that the above views regarding the distributions of the monsoon regions
483 and arid zone in Asia before the TP uplift have limitations and uncertainties. First, in this
484 simplified experiment, we look at a condition with zero global topography globally, which is
485 unrealistic for almost any geological period. Also, in our study, as well as in many other previous
486 numerical simulations, the same present-day land-ocean configuration has been used, while in fact
487 global distribution pattern of land masses and oceans changed greatly during the Cenozoic due to
488 plate tectonics [36,76]. The position of the Eurasia continent, especially the position of the Indian
489 subcontinent [77], and the condition of the Tethys Sea [78,79] were very different from the
490 present. Earlier numerical simulations have indicated that changes in land-ocean configuration,
491 especially such changes in the lower latitudes, may significantly influence the establishment and
492 evolution of the monsoon climates [23,24,55,80]. Therefore, there is the urgent need to study the
493 influence of the geologically realistic distribution pattern of land masses and oceans on the
494 formation of Asian monsoons before the TP uplift.

495 Second, changing atmospheric CO₂ concentration was not considered in our numerical
496 simulations. Atmospheric CO₂ concentration changed significantly during the Cenozoic [81]. A
497 recent simulation study by Licht *et al.* [41] revealed that the Asian monsoons had already
498 appeared in the late Eocene, which was likely the result of the enhanced greenhouse effect from
499 extremely high atmospheric CO₂ concentrations at the time. However, according to the IPCC's
500 projections for future climate change scenarios based on multi-model ensembles [82], although
501 precipitation may increase in the Asian monsoon regions under the scenario of increased
502 greenhouse gas concentrations, mostly caused by enhanced moisture convergence, the monsoon
503 circulation intensity itself will be weakened. This means that the effects of changing atmospheric
504 CO₂ concentration on the Asian monsoons before the TP uplift should also be examined in detail.
505 Additionally, making things even more complex, the palaeogeography related to plate tectonics
506 has been recognized as a key factor controlling the long-term evolution of the atmospheric CO₂
507 through its capability of modulating the efficiency of silicate weathering and the climate
508 sensitivity to atmospheric CO₂ [83]. Consequently, the modulation of changing atmospheric CO₂
509 to the development of the Asian monsoons during geologic time has been identified as an
510 important area for further research.

511 Finally, in view of the current limited knowledge and the importance in understanding the
512 distribution of the Asian monsoon and arid regions before the TP uplift as the foundation for the
513 study of the impact of the TP uplift on spatial patterns of climates in Asia, there is much more to
514 accomplish in areas of numerical simulation and analysis of geological records. This is especially
515 true in terms of cross-comparison and integration of the simulation results and geological evidence.
516 For example, regarding the question of whether the EAM existed before the Miocene, or if it
517 indeed existed back then, its spatial range and intensity are still open for answers. From the
518 modeling perspective, the emergence of the SAM should be earlier than that of the EAM, which,
519 however, still lacks supporting geological evidence at the present. Unless the paleoelevation of the
520 TP was sufficiently high in the Paleocene-Eocene period, the EAM system would not have been
521 established at a much earlier time than the Miocene. For future studies, in the Tertiary before the
522 TP uplift or when the plateau elevation was still low, the question of whether there existed a
523 quasi-monsoon zone in the mid- to high-latitudes of Eurasia, separated from the tropical and
524 subtropical circulations, also requires cross-validation using relevant geological records. Although

525 there should have been no strong aridity in the mid-latitude Asian inland north of 40°N before the
526 TP uplift according to numerical simulations, the actual timing of formation and spatio-temporal
527 evolution history of the mid-latitude arid regions in central Asia remain as important scientific
528 questions that require validation using reliable high-resolution geological records.

529

530 FUNDING

531 The work was supported by the Strategic Priority Research Program of the Chinese Academy
532 of Sciences (XDB03020601) and the National Natural Science Foundation of China (41290255)
533 with numerical modelling support from NCAS-Climate and NCAS-CMS in the UK.

534

535 REFERENCES

- 536 1. Liu, TS. *Loess and the Environment*. Beijing: China Ocean Press, 1985; 251.
- 537 2. An, ZS. 2014. *Late Cenozoic Climate Change in Asia: Loess, Monsoon and Monsoon-Arid*
538 *Environment Evolution*. Dordrecht, Neth.: Springer, 2014; 582.
- 539 3. Kroon, D, Steens, TN and Troelstra, RT. Onset of monsoonal related upwelling in the western
540 Arabian Sea. In Prell, WL and Niitsuma, N *et al. Proceedings of the Ocean Drilling Program.*
541 *Scientific Results* 1991; **117**: 257–263.
- 542 4. Quade, J, Cerling, TE and Bowman, JR. Development of Asian monsoon revealed by marked
543 ecological shift during the Latest Miocene in northern Pakistan. *Nature* 1989; **342**: 163–166.
- 544 5. Gupta, SM. Indian monsoon cycles through the last twelve million years. *Earth Sci India*
545 2010; **3**: 248–280.
- 546 6. Gupta, AK, Yuvaraja, A and Prakasam, M *et al.* Evolution of the South Asian monsoon wind
547 system since the late Middle Miocene. *Palaeogeogr Palaeoclimatol Palaeoecol* 2015; **438**:
548 160–167.
- 549 7. Ding, Z, Rutter, NW and Han, J *et al.* A coupled environmental system formed at about 2.5
550 Ma over East Asia. *Palaeogeogr Palaeoclimatol Palaeoecol* 1992; **94**: 223–242.
- 551 8. Liu, TS and Ding, ZL. Chinese loess and the paleomonsoon. *Ann Rev Earth Planet Sci* 1998;
552 **26**: 111–145.
- 553 9. An, ZS, The history and variability of the East Asian paleomonsoon climate. *Quat Sci Rev*
554 2000; **19**: 171–187.
- 555 10. Sun, D, Shaw, J and An, Z *et al.* Magnetostratigraphy and paleoclimatic interpretation of a
556 continuous 7.2 Ma Late Cenozoic eolian sediments from the Chinese Loess Plateau. *Geophys*
557 *Res Lett* 1998; **25**: 85–88.
- 558 11. Ding, Z, Sun, J and Yang, S *et al.* Preliminary magnetostratigraphy of a thick eolian red
559 clay-loess sequence at Lingtai, the Chinese Loess Plateau. *Geophys Res Lett* 1998; **25**: 1225–
560 1228.
- 561 12. Guo, ZT, Ruddiman, WF and Hao, QZ *et al.* Onset of Asian desertification by 22 Myr ago
562 inferred from loess deposits in China. *Nature* 2002; **416**: 159–163.
- 563 13. Qiang, XK, An, ZS and Song, YG *et al.* New eolian red clay sequence on the western
564 Chinese Loess Plateau linked to onset of Asian desertification about 25 Ma ago. *Science*
565 *China Earth Sciences* 2011; **54**:136–144.
- 566 14. Sun, XJ and Wang, PX. How old is the Asian monsoon system? — Palaeobotanical records
567 from China. *Palaeogeogr Palaeoclimatol Palaeoecol* 2005; **222**: 181–222.
- 568 15. Guo, ZT, Sun, B and Zhang, ZS *et al.* A major reorganization of Asian climate regime by the

- 569 early Miocene. *Clim Past* 2008; **4**: 153–174.
- 570 16. Wang, PX, Wang, B and Cheng H *et al.* The global monsoon across timescales: coherent
571 variability of regional monsoons. *Climat Past*, 2014; **10**: 2007–2052.
- 572 17. Rea, DK. The paleoclimatic record provided by eolian deposition in the deep sea: the
573 geologic history of wind. *Rev Geophys* 1994; **32**: 159–195.
- 574 18. Rea, DK, Snoeckx, H and Joseph, LH. Late Cenozoic eolian deposition in the North Pacific:
575 Asian drying, Tibetan up lift and cooling of the Northern Hemisphere. *Paleoceanography*
576 1998; **13**: 215–224.
- 577 19. Sun, JM, Ye, J, Wu, WY *et al.* Late Oligocene-Miocene mid-latitude aridification and wind
578 patterns in the Asian interior. *Geology* 2010; **38**: 515–518.
- 579 20. Quan, C, Liu, Z, Utescher, T *et al.* Revisiting the Paleogene climate pattern of East Asia: a
580 synthetic review. *Earth-Sci Rev* 2014; **139**: 213–230.
- 581 21. Webster, PJ. The elementary monsoon. In: Fein, JS and Stephens, PL (eds.). *Monsoons*.
582 New York: John Wiley, 1987; 3–32.
- 583 22. Young, JA. Physics of monsoons: The current view. In: Fein, JS and Stephens, PL (eds.).
584 *Monsoons*. New York: John Wiley, 1987; 211–243.
- 585 23. Dirmeyer, PA. Land–sea geometry and its effect on monsoon circulations. *J Geophys Res*
586 1998; **103**: 11555–11572.
- 587 24. Chou, C. Land–sea heating contrast in an idealized Asian summer monsoon. *Clim Dyn* 2003;
588 21: 11–25.
- 589 25. Hahn, DG and Manabe, S. The role of mountains in the south Asian monsoon circulation. *J*
590 *Atmos Sci* 1975; **32**: 1515–1541.
- 591 26. Kutzbach, JE, Prell, WL and Ruddiman, WF. Sensitivity of Eurasian climate to surface uplift
592 of the Tibetan plateau. *J Geol* 1993; **101**: 177–190.
- 593 27. Liu, XD and Yin, ZY. Sensitivity of East Asian monsoon climate to the uplift of the Tibetan
594 Plateau. *Palaeogeogr Palaeoclimatol Palaeoecol* 2002; **183**: 223–245.
- 595 28. Boos, WR and Kuang, ZM. Dominant control of the South Asian monsoon by orographic
596 insulation versus plateau heating. *Nature* 2010; **463**: 218–22.
- 597 29. Chao, WC and Chen, BD. The origin of monsoon. *J Atmos Sci* 2001; **58**: 3497–3507.
- 598 30. Manabe, S and Broccoli, AJ. Mountains and arid climates of middle latitudes. *Science* 1990;
599 **247**: 192–194.
- 600 31. Ramstein, G, Fluteau, F and Besse, J *et al.* Effect of orogeny, plate motion and land–sea
601 distribution on Eurasian climate change over the past 30 million years. *Nature* 1997; **386**:
602 788–795.
- 603 32. Zhang, ZS, Wang, HJ and Guo, ZT *et al.* What triggers the transition of palaeoenvironmental
604 patterns in China, the Tibetan Plateau uplift or the Paratethys Sea retreat? *Palaeogeogr*
605 *Palaeoclimatol Palaeoecol* 2007; **245**: 317–331.
- 606 33. Shi, ZG, Liu, XD and An, ZS *et al.* Simulated variations of eolian dust from inner Asian
607 deserts during late Pliocene-Pleistocene periods. *Climate Dynamics* 2011; **37**: 2289–2301.
- 608 34. Ruddman, WF and Kutzbach, JE. Plateau uplift and climatic change. *Sci American* 1991; **264**:
609 66–75.
- 610 35. Clift, PD, Hodges, KV and Heslop, D *et al.* Correlation of Himalayan exhumation rates and
611 Asian monsoon intensity. *Nature Geoscience* 2008; **1**: 875–880.
- 612 36. Chatterjee, S, Goswami, A and Scotese, CR. The longest voyage: tectonic, magmatic, and
613 paleoclimatic evolution of the Indian plate during its northward flight from Gondwana to

- 614 Asia. *Gondwana Research* 2013; **23**: 238-267.
- 615 37. Wang, GC, Cao, K and Zhang KX *et al.* Spatio-temporal framework of tectonic uplift stages
616 of the Tibetan Plateau in Cenozoic. *Sci China Earth Sci* 2011; **54**: 29-44.
- 617 38. Wang, C, Dai, J and Zhao, X *et al.* Outward-growth of the Tibetan Plateau during the
618 Cenozoic: A review. *Tectonophysics* 2014; **621**: 1-43.
- 619 39. An, ZS, Kutzbach, JE and Prell, WL *et al.* Evolution of Asian monsoons and phased uplift of
620 the Himalaya-Tibetan Plateau since Late Miocene times. *Nature*, 2001; **411**: 62-66.
- 621 40. Huber, M and Goldner, A. Eocene monsoons. *J Asian Earth Sci* 2012; **44**: 3-23.
- 622 41. Licht, A, Van Cappelle, M and Abels, H *et al.* Asian monsoons in a late Eocene greenhouse
623 world. *Nature*, 2014; **513**: 501-506.
- 624 42. Liu, XD, Sun, H and Miao, YF *et al.* Impacts of uplift of northern Tibetan Plateau and
625 formation of Asian inland deserts on regional climate and environment. *Quat Sci Rev* 2015;
626 **116**: 1-14.
- 627 43. Gordon, C, Cooper, C and Senior C *et al.* The simulation of SST, sea ice extents and ocean
628 heat transports in a version of the Hadley Centre coupled model without flux adjustments.
629 *Clim Dyn* 2000; **16**:147-16.
- 630 44. Jones, C, Gregory, J and Thorpe, R *et al.* Systematic optimisation and climate simulation of
631 FAMOUS, a fast version of HadCM3. *Climate Dynamics* 2005; **25**: 189-204.
- 632 45. Smith, RS, Gregory, JM and Osprey, A. A description of the FAMOUS (version XDBUA)
633 climate model and control run. *Geoscientific Model Development* 2008; **1**: 53-68.
- 634 46. Smith, R. The FAMOUS climate model (versions XFXWB and XFHCC): description update
635 to version XDBUA. *Geoscientific Model Development*, 2012; **5**: 269-276.
- 636 47. Wang, B and Ding, Q. Changes in global monsoon precipitation over the past 56 years.
637 *Geophys Res Lett* 2006; **33**: doi:10.1029/2005GL025347.
- 638 48. Ramage, CS. *Monsoon Meteorology*. New York and London: Academic Press, 1971.
- 639 49. Warner, TT. *Desert meteorology*. Cambridge University Press, 2004.
- 640 50. Nicholson, SE. *Dryland climatology*. Cambridge University Press, 2011.
- 641 51. McIlveen, R. *Fundamentals of weather and climate*. Psychology Press, 1992.
- 642 52. Zhao, SQ. A new scheme for comprehensive geographical regionalization in China. *Acta*
643 *Geographica Sinica* 1983; **38**: 1-10.
- 644 53. Geng, QL, Wu, PT and Zhang, QF *et al.* Dry/wet climate zoning and delimitation of arid
645 areas of Northwest China based on a data-driven fashion. *J Arid Land* 2014; **6**: 287-299.
- 646 54. Zhang, Z., Flatøy, F and Wang, H *et al.* Early Eocene Asian climate dominated by desert and
647 steppe with limited monsoons. *J Asian Earth Sci* 2012; **44**: 24-35.
- 648 55. Xu, Z, Fu, C and Qian, Y. Relative roles of land-sea distribution and orography in Asian
649 monsoon intensity. *J Atmos Sci* 2009; **66**: 2714-2729.
- 650 56. Wu, G, Liu, Y and Dong B *et al.* Revisiting Asian monsoon formation and change associated
651 with Tibetan Plateau forcing: I. Formation. *Climate dynamics* 2012; 39: 1169 -1181.
- 652 57. Quan, C, Liu, YSC and Utescher, T. Paleogene evolution of precipitation in northeast China
653 supporting the middle Eocene intensification of the East Asian monsoon. *Palaios* 2011; **26**:
654 743-753.
- 655 58. Chung, S, Lo, CH and Lee TY *et al.* Diachronous uplift of the Tibetan plateau starting 40
656 Myr ago. *Nature* 1998; **394**: 769-773.
- 657 59. Tapponnier, P, Xu, ZQ and Rogerm, F *et al.* Geology - Oblique stepwise rise and growth of
658 the Tibetan Plateau. *Science* 2001; **294**: 1671-1677.

- 659 60. Liu, XD and Dong, BW. Influence of the Tibetan Plateau uplift on the Asian monsoon-arid
660 environment evolution. *Chin Sci Bull* 2013; **58**: 4277-4291.
- 661 61. Quade, J, Breecker, DO and Daëron, M *et al.* The paleoaltimetry of Tibet: An isotopic
662 perspective. *Amer J Sci* 2011; **311**: 77–115.
- 663 62. Xiao, G, Guo, Z and Dupont-Nivet, G *et al.* Evidence for northeastern Tibetan Plateau uplift
664 between 25 and 20Ma in the sedimentary archive of the Xining Basin, Northwestern China.
665 *Earth Planet Sci Lett* 2012; **317**: 185–195.
- 666 63. Ding, L, Xu, Q and Yue, Y *et al.* The Andean-type Gangdese Mountains: Paleoelevation
667 record from the Paleocene–Eocene Linzhou Basin. *Earth Planet Sci Lett* 2014; **392**: 250–264.
- 668 64. Wang, J, Wang, YJ and Liu, ZC *et al.* Cenozoic environmental evolution of the Qaidam Basin
669 and its implications for the uplift of the Tibetan Plateau and the drying of central Asia.
670 *Palaeogeogr Palaeoclimatol Palaeoecol* 1999; **152**: 37–47.
- 671 65. Miao, Y, Fang, X and Song, Z *et al.* Late Eocene pollen records and palaeoenvironmental
672 changes in northern Tibetan Plateau. *Sci China Series D: Earth Sci* 2008; **51**: 1089–1098.
- 673 66. Fang, X., Zan, J., Appel, E *et al.* An Eocene–Miocene continuous rock magnetic record from
674 the sediments in the Xining Basin, NW China: indication for Cenozoic persistent drying
675 driven by global cooling and Tibetan Plateau uplift. *Geophys J Intern* 2015; **201**: 78–89.
- 676 67. Broccoli, AJ and Manabe, S. The effects of orography on midlatitude northern hemisphere
677 dry climates. *J Clim* 1992; **5**: 1181–1201.
- 678 68. Sun, J, Ni, X and Bi, S *et al.* Synchronous turnover of flora, fauna, and climate at the Eocene-
679 Oligocene Boundary in Asia. *Scientific reports* 2014; **4**: 7463, doi:10.1038/srep07463.
- 680 69. Srivastava, G, Spicer, RA and Spicer, TEV *et al.* Megafloora and palaeoclimate of a Late
681 Oligocene tropical delta, Makum Coalfield, Assam: Evidence for the early development of
682 the South Asia Monsoon. *Palaeogeogr Palaeoclimatol Palaeoecol* 2012; **342**: 130–142.
- 683 70. Licht, A, Boura, A and De Franceschi, D *et al.* Late middle Eocene fossil wood of Myanmar:
684 Implications for the landscape and the climate of the Eocene Bengal Bay. *Rev Palaeobotany*
685 *Palynology* 2015; **216**: 44–54.
- 686 71. Wang, P. Neogene stratigraphy and paleoenvironments of China. *Palaeogeogr*
687 *Palaeoclimatol Palaeoecol* 1990; **77**: 315–334.
- 688 72. Liu, TS and Guo, ZT. Geological environment in China and global change, in: An, ZS (ed.).
689 *Selected Works of Liu Tungsheng*. Beijing: Science Press, 1997, 192–202.
- 690 73. Rowley DB and Currie BS. Palaeo-altimetry of the late Eocene to Miocene Lunpola basin,
691 central Tibet. *Nature* 2006; **439**: 677-681.
- 692 74. Gupta, AK, Singh, RK and Joseph, S *et al.* Indian Ocean high-productivity event (10–8 Ma):
693 linked to global cooling or to the initiation of the Indian monsoons? *Geology* 2004; **32**: 753–
694 756.
- 695 75. Huang, Y, Clemens, SC and Liu, W *et al.* Large-scale hydrological change drove the late
696 Miocene C4 plant expansion in the Himalayan foreland and Arabian Peninsula. *Geology*
697 2007; **35**: 531–534.
- 698 76. Ali, JR and Aitchison, JC. Gondwana to Asia: Plate tectonics, paleogeography and the
699 biological connectivity of the Indian sub-continent from the Middle Jurassic through latest
700 Eocene (166–35 Ma). *Earth-Sci Rev* 2008; **88**: 145–166.
- 701 77. Molnar, P and Stock, JM. Slowing of India's convergence with Eurasia since 20 Ma and its
702 implications for Tibetan mantle dynamics. *Tectonics* 2009; **28**: TC3001, doi:10.1029/
703 2008TC002271

- 704 78. Bosboom, RE, Dupont-Nivet, G and Houben, AJP *et al.* Late Eocene sea retreat from the
705 Tarim Basin (west China) and concomitant Asian paleoenvironmental change. *Palaeogeogr*
706 *Palaeoclimatol Palaeoecol* 2011; **299**: 385–398.
- 707 79. Bosboom, R, Dupont-Nivet, G and Grothe, A *et al.* Timing, cause and impact of the late
708 Eocene stepwise sea retreat from the Tarim Basin (west China). *Palaeogeogr Palaeoclimatol*
709 *Palaeoecol* 2014; **403**: 101-118.
- 710 80. Liang, X, Liu, Y and Wu, G. The role of land-sea distribution in the formation of the Asian
711 summer monsoon. *Geophys Res Lett* 2005; **32**: L03708, doi:10.1029/2004GL021587.
- 712 81. Beerling, DJ and Royer, DL. Convergent cenozoic CO₂ history. *Nature Geoscience* 2011; **4**:
713 418–420.
- 714 82. Christensen, JH, Hewitson, B and Busuioc A *et al.* Regional Climate Projections. In:
715 Solomon, S (ed.). *Climate change 2007: the physical science basis: Working group I*
716 *contribution to the fourth assessment report of the IPCC*. Cambridge: Cambridge University
717 Press, 2007; 847–940.
- 718 83. Godd ris, Y, Donnadieu, Y and Le Hir, G *et al.* The role of palaeogeography in the
719 Phanerozoic history of atmospheric CO₂ and climate. *Earth-Sci Rev* 2014; **128**: 122–138.
720